Microwave Image Reconstruction with Two-Antenna Aperture Synthesis and Spatial Antennas Separation

V. Semenchik [1)], V. Pahomov [2)]

1) Belarussian State University, 4, Nezavisimosti Avenue, Minsk, 220050, Belarus,
phone/Fax: 375 (17) 277-08-90, E-mail: semenchik@bsu.by

Abstract: Two-antenna aperture synthesis scanning doubles azimuth resolution of imaging systems. Our previously reported image reconstruction approach assumes that transmitting and receiving antennas are situated closely to each other, but in real conditions this can be violated due to antennas physical dimensions and necessity of coupling reducing. Using common approaches can cause reconstructed image distortions. This paper presents approach that takes into account antennas separation. Effectiveness of the approach is experimentally proven.

Keywords: Microwave imaging, Two-antenna Aperture Synthesis

INTRODUCTION

Microwave imaging is a set of methods for obtaining hidden object images with microwave field. The region of interest with object in it is illuminated with microwaves, then reflected field is measured and processed to obtain object image. Microwave imaging has a lot of applications: ground penetrating radars (GPRs) for landmine and underground utility detection and geological surveys, nondestructive testing, medicine etc.

Two-antenna scan aperture synthesis is well-known technique used to improve system spatial resolution [1]. Recently we presented an approach for two-antenna scan for microwave imaging [2]. The approach uses an assumption that receiving and transmitting antennas are separated in the same point. But limited antennas physical dimensions and necessity of coupling reducing does not allow placing antennas too close. Using the approach that does not take into account antennas separation can cause distortions in reconstructed image.

This paper presents an approach to microwave image reconstruction with two-antenna scan aperture synthesis that deals with antennas separation. An approach solves linearized (with Born approximation) inverse problem in frequency domain. Closed form frequency response was obtained under certain approximations, but numerical simulations and experiments have showed that using numerically calculated frequency response results in better reconstructed image quality.

PHYSICAL MODEL

The physical model diagram for two-antenna scan aperture synthesis is presented in figure 1. The object is assumed to be plain for simplicity; however, three-dimensional prominent objects can be divided into such plane "slices".

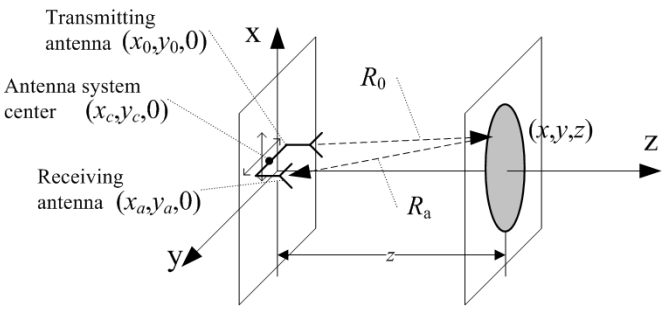

Fig.1 – Two-antenna scan aperture synthesis diagram

Note that in this scanning scheme, incident field on object surface is constantly changing with antennas movement, so the data gathered isn't static field distribution in aperture plane.

Antenna coordinates are linked with the following equation:

$$\begin{cases} x_0 = x_c + \Delta x \\ y_0 = y_c + \Delta y \end{cases} \quad \begin{cases} x_a = x_c - \Delta x \\ y_a = y_c - \Delta y \end{cases}, \tag{1}$$

where x_0 and y_0 are transmitting antenna coordinates, x_a and y_a are receiving antenna coordinates, and x_c and y_c are antenna system center coordinates.

According to Kirchoff assumption, complex amplitude of field reflected from the object in point (x, y) directly on object surface can be expressed as

$$\begin{aligned} \dot{p}(x,y,0) &= \dot{p}_0(x,y,0)\cdot\dot{K}(x,y) = \\ &= \dot{p}_T(x-x_0, y-y_0, z)\cdot\dot{K}(x,y), \end{aligned} \tag{2}$$

where $\dot{p}(x,y,0)$ is reflected field amplitude, $\dot{p}_0(x,y,0)$ is incident field amplitude at the same point, $\dot{K}(x,y)$ is object reflection coefficient at the same point. Expression $\dot{p}_T(x,y,z)$ generalizes incident field and describes amplitude of transmitting antenna field when no scatterers are present and transmitting antenna is situated at zero point.

According to Born approximation [3], which is applicable to strongly scattering plane objects in this case [2], the field that is reflected to the aperture plane can be expressed as follows:

$$\dot{p}(x_a,y_a,z) = \int_{-\infty}^{\infty}\int_{-\infty}^{\infty} \dot{p}(x,y,0)\,\dot{p}_O(x_a-x, y_a-y, z)\,dxdy, \tag{3}$$

where $\dot{p}_0(x,y,z)$ is scattered field from single scatterer (object point).

Substituting object surface field from expression (2) to expression (3) we obtain

$$\dot{p}(x_a, y_a, z) =$$

$$= \int_{-\infty}^{\infty}\int_{-\infty}^{\infty} \dot{K}(x,y)\cdot \dot{p}_T(x-x_0, y-y_0, z)\cdot \dot{p}_0(x_a-x, y_a-y, z)\,dxdy = \quad (4)$$

$$= \int_{-\infty}^{\infty}\int_{-\infty}^{\infty} \dot{K}(x,y)\cdot h_Z(x-x_c, y-y_c)\,dxdy,$$

where $h_Z(x-x_c, y-y_c)$ is system impulse response,

$$h_Z(x-x_c, y-y_c) =$$
$$= p_T\left([x-x_c]+\Delta x, [y-y_c]+\Delta y, z\right)\times$$
$$\times p_O\left(-[x-x_c]-\Delta x, -[y-y_c]-\Delta y, z\right).$$

Considering both transmitting antenna and object point small enough, the field can be treated as spherical wave field. Thus

$$\dot{p}_T(x-x_0, y-y_0, z) = \frac{\exp(ikR_0)}{R_0},$$
$$p_0(x_a-x, y_a-y, z) = \frac{\exp(ikR_a)}{R_a}. \quad (5)$$

where $R_0 = \sqrt{(x-x_0)^2+(y-y_0)^2+z^2}$,

$R_a = \sqrt{(x-x_a)^2+(y-y_a)^2+z^2}$.

Combining expressions (5) and (4) we finally get

$$\dot{p}(x_a, y_a, z) = \int_{-\infty}^{\infty}\int_{-\infty}^{\infty} \dot{K}(x,y)\cdot\frac{\exp(ikR_0)}{R_0}\cdot\frac{\exp(ikR_a)}{R_a}\,dxdy =$$
$$\int_{-\infty}^{\infty}\int_{-\infty}^{\infty} \dot{K}(x,y)\cdot h(x-x_c, y-y_c, z)\,dxdy. \quad (6)$$

The equation (6) is the key to image reconstruction. It's Fredholm integral equation of the first kind with difference kernel, and it can be solved in frequency domain [4]. The solution is as follows (it omits regularization issues for simplicity):

$$\dot{K}(x,y) = \mathbf{F}^{-1}_{\omega,\xi}\left[\frac{\mathbf{F}_{x_a,y_a}\left[p(x_a, y_a, z)\right]}{\mathbf{F}_{x,y}\left[h(x,y,z)\right]}\right], \quad (7)$$

where $\mathbf{F}_{x,y}[\ ]$ denotes two-dimensional direct Fourier transform with respect to coordinates x and y, and $\mathbf{F}^{-1}_{\omega,\xi}[\ ]$ denotes two-dimensional inverse Fourier transform with respect to coordinates ω and ξ.

To obtain the solution, we need to calculate the Fourier transform of equation kernel, which is system frequency response:

$$\dot{H}(\omega,\zeta) = \mathbf{F}_{x,y}\left[h(x,y,z)\right] = \mathbf{F}_{x,y}\left[\frac{\exp(ikR')}{R'}\cdot\frac{\exp(ikR'')}{R''}\right], \quad (8)$$

where

$R' = \sqrt{(x+\Delta x)^2+(y+\Delta y)^2+z^2}$,

$R'' = \sqrt{(x-\Delta x)^2+(y-\Delta y)^2+z^2}$.

However, it's not possible to obtain close form of transform (8) in general case.

NUMERICAL FREQUENCY RESPONSE CALCULATION

Discrete Fourier transform algorithms can be used to calculate frequency response. In this case, choosing appropriate limits and sampling interval for kernel discrete values calculation should be considered.

Both range and sampling step determine frequency values corresponding to frequency samples after DFT calculation. These values should correspond to frequency samples of measured data DFT, in order to perform element-by-element division according to equation (7).

But, frequencies of discrete field spectrum are determined by aperture size and sampling step. Thus, kernel should be sampled exactly in the same points as aperture does.

On the other hand, limiting kernel sampling range will result in frequency response distortion, since DFT results in convolution of "true" kernel spectrum and spectrum of rectangular window equal to sampling range. Practically to avoid these distortions, kernel sampling range should be much more that aperture size.

To resolve this contradiction, kernel sampling range is chosen to be multiple of aperture size, and sampling step coincides with aperture's one. In this case, each n-th (n is multiply order) sample of frequency response coincides to measured data spectrum sample. This is schematically shown for $n = 2$ in fig. 2.

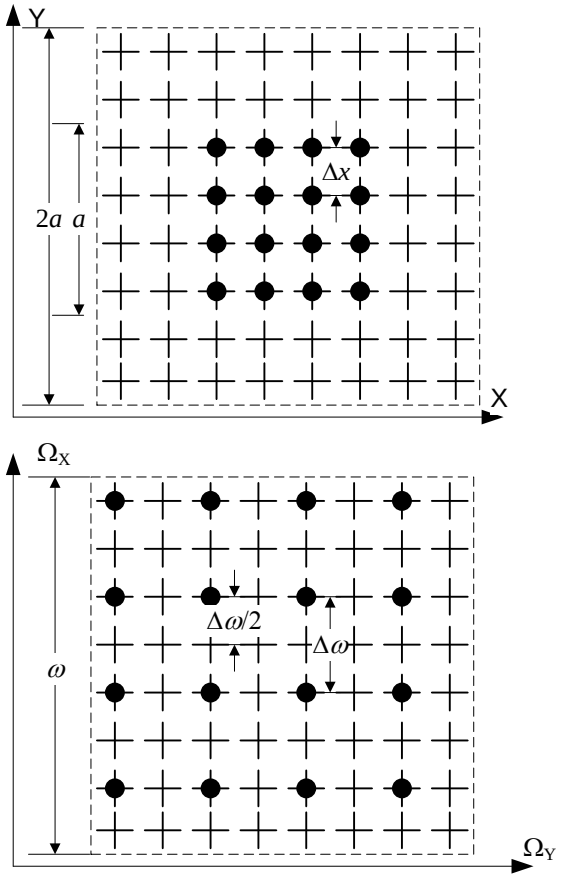

Fig 2. Kernel sampling scheme

Upper image shows kernel samples (crosses) and measured data samples (circles) in spatial domain, while lower shows the same in frequency domain. Notation is: a – aperture size, Δx – spatial sampling step, $\omega = 2\pi/\Delta x$ – frequency domain range, $\omega = 2\pi/a$ – frequency domain sampling step.

CLOSED FORM SOLUTION

Obtaining closed-form solution under certain approximations is of interest e.g. for analyze purposes. Considering $x \ll z$, $y \ll z$ equations for R' and R'' can be approximated with Taylor series trimmed on quadratic terms:

$$R' \approx z + \frac{1}{2z}\left[(x+\Delta x)^2 + (y+\Delta y)^2\right] = \\ = z + \frac{1}{2z}\left[x^2 + y^2 + \Delta x^2 + \Delta y^2\right] + \frac{1}{z}\left[x\Delta x + y\Delta y\right], \quad (9)$$

$$R'' \approx z + \frac{1}{2z}\left[(x-\Delta x)^2 + (y-\Delta y)^2\right] = \\ = z + \frac{1}{2z}\left[x^2 + y^2 + \Delta x^2 + \Delta y^2\right] - \frac{1}{z}\left[x\Delta x + y\Delta y\right]. \quad (10)$$

Assuming

$$R = \sqrt{x^2+y^2+z^2} \approx z + \frac{1}{2z}\left[x^2 + y^2 + \Delta x^2 + \Delta y^2\right] = \\ = z + \frac{\Delta x^2 + \Delta y^2}{2z} + \frac{1}{2z}\left[x^2 + y^2\right] \approx \sqrt{x^2 + y^2 + \left(z + \frac{\Delta x^2 + \Delta y^2}{2z^2}\right)} \quad (11)$$

we can write that

$$R' \approx R + \frac{1}{z}\left[x\Delta x + y\Delta y\right], \\ R'' \approx R - \frac{1}{z}\left[x\Delta x + y\Delta y\right]. \quad (12)$$

In that case, system impulse response can be written as

$$h(x,y) = \frac{\exp(ikR')}{R'} \cdot \frac{\exp(ikR'')}{R''} \approx \\ \approx \frac{\exp\left[ik\left(R + \frac{1}{2}(x\Delta x + y\Delta y)\right)\right]\exp\left[ik\left(R - \frac{1}{2}(x\Delta x + y\Delta y)\right)\right]}{\left(R + \frac{1}{2}(x\Delta x + y\Delta y)\right)\left(R - \frac{1}{2}(x\Delta x + y\Delta y)\right)} = \\ = \frac{\exp(2ikR)}{\left(R + \frac{1}{2}(x\Delta x + y\Delta y)\right)\left(R - \frac{1}{2}(x\Delta x + y\Delta y)\right)}. \quad (13)$$

Because of initial assumptions, both multipliers in denominator of expression (13) can be replaced either with R or with z (because $R \approx z$), and we finally obtain that

$$h(x,y) \approx \frac{1}{z}\frac{\exp(2ikR)}{R}. \quad (14)$$

If we add $\lambda \ll z$ condition to above, we can calculate Fourier transform on expression (14) [5], and it can be written as (without scale multipliers):

$$H(\omega,\zeta) = \exp\left(i\left[z + \frac{\Delta x^2 + \Delta y^2}{2z^2}\right]\sqrt{4k^2 - \omega^2 - \xi^2}\right). \quad (15)$$

It's interesting to note that expression (14) describes impulse response (Fredholm equation kernel) of an imaging system that differs from one being considered in three points:

1. It performs one-antenna scan rather than two-antenna scan
2. The illuminating wave frequency is doubled
3. The distance between object and aperture plane is $z + \frac{\Delta x^2 + \Delta y^2}{2z^2}$ rather than z.

Comparing this to previously reported approach [2], we can state that antennas separation result in focusing plane displacement.

It's worth estimating the roughness of conditions assumed: $x \ll z$, $y \ll z$ and $\lambda \ll z$, since they're not always accomplished. The estimating is hardly possible in general case, but it becomes possible when antennas are situated closely enough. The kernel in equation (6) is written as follows in this case (note that assumptions mentioned above are omitted):

$$\dot{h}(x,y) = \frac{\exp(2ikR)}{R^2}, \quad (16)$$

where $R = \sqrt{x^2 + y^2 + z^2}$.

Let's multiply this kernel to the following value. It can be shown that this value is almost constant even when assumptions mentioned above are omitted.

$$\dot{b} = \left(1 - \frac{1}{2ikR}\right). \quad (17)$$

After some transformations we obtain

$$\dot{h}'(x,y) = \frac{\exp(2ikR)}{R^2}\left(1 - \frac{1}{2ikR}\right) = -\frac{1}{2ikz}\frac{\partial}{\partial z}\frac{\exp(2ikR)}{R}. \quad (18)$$

Closed-form Fourier transform can be calculated for the expression (18):

$$\dot{H}(\omega,\xi) = -\frac{1}{2ikz}\exp\left(iz\sqrt{4k^2 - \omega^2 - \omega_y^2}\right). \quad (19)$$

On the other hand, closed-form frequency response (15) will be written as follows in this case:

$$H(\omega,\zeta) = \exp\left(iz\sqrt{4k^2 - \omega^2 - \xi^2}\right). \quad (20)$$

Comparing expressions (19) and (20), we come to the fact that closed form of frequency response can be used even when conditions introduced are violated, considering transmitting and receiving antennas are close enough.

NUMERICAL SIMULATIONS

Numerical simulations were performed to test algorithm proposed. Also, numerical simulations showed whether closed form frequency response is effective when antennas are spatially separated and conditions introduced are violated. Simulations consisted in scattered field calculation and image reconstruction with algorithm proposed followed.

Simulation conditions were chosen to match experimental setup [6] parameters so that numerical simulation and experimental data are comparable. Square system aperture had 32-by-32 points situated at rectangular grid nodes with 1 cm sampling step.

A point object was situated below the center of the aperture. The distance between object and the aperture was 15cm. Antennas separation was altered from $\Delta y = 0$ to $\Delta y = 10$cm, Δx was always zero. 10GHz illumination frequency was chosen.

Figure 3 shows object image reconstructed without taking care of antennas separation, and it reflects distortions caused by separation. Upper figure (3a) shows object image for $\Delta y = 10$cm, while lower figure (3b) shows image slice along Y axis for different Δy values. Displacement values are shown in legend (in centimeters). Slice position is marked in object image with vertical dashed line.

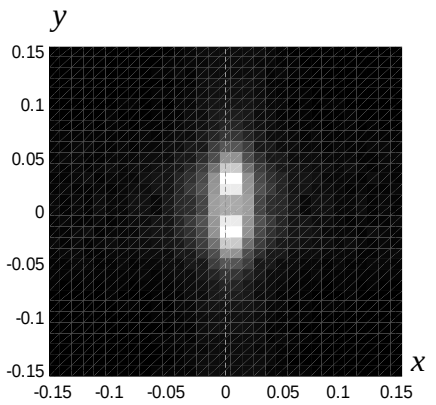

a)

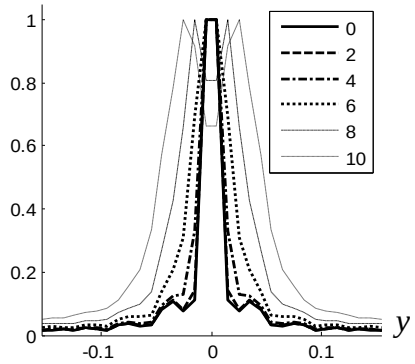

b)

Fig. 3. Point object image reconstructed without taking into account antenna separation

Figure 3 shows that image distortions became significant for $\Delta y = 6$cm, that is, when antennas displacement ($2\Delta y$) approaches distance to the object. Additional simulation was performed to this assumption. In this simulation the distance to the object was reduced to 6cm. Figure 4 shows vertical slices of images reconstructed for different Δy values.

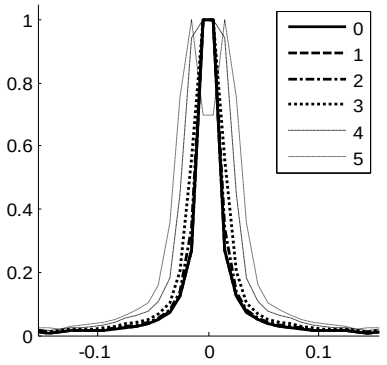

Fig. 4. Vertical slice of point object image reconstructed when distance to object is 6 cm.

It's seen that image distortions became significant when antennas displacement become 8cm ($\Delta y = 4$cm). This proves assumption proposed.

Figure 5 shows images reconstructed using approach proposed for maximum antennas displacement ($\Delta y = 10$cm). Upper image (5a) is obtained with numerical frequency response while lower one (5b) is with closed form response.

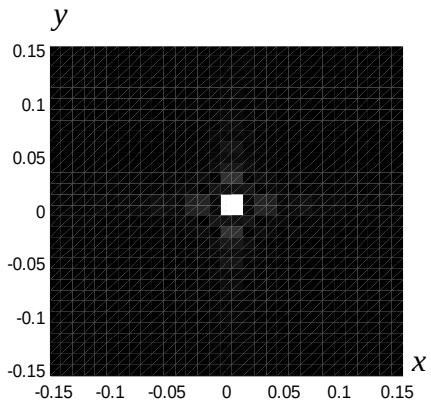

a)

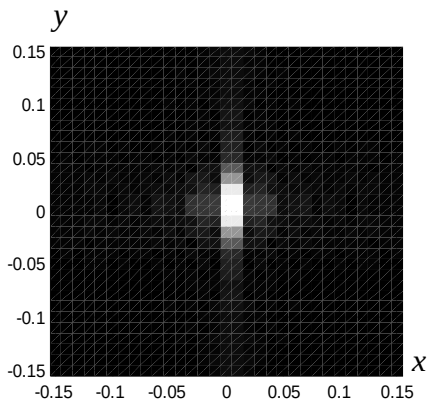

b)

Fig. 5. Point object image reconstructed with approach proposed

It's seen that image distortions caused by antennas separation are almost totally disappear when numerical frequency response is used. With closed form frequency response, the distortions retain noticeable though they're reduced significantly.

Additional simulations were performed to test the approach in multi-frequency case [2, 6]. Eleven illumination frequencies from 6.0 GHz to 10.0 GHz were used. Image reconstruction results for multi-frequency case are shown in figure 6. Antenna displacement was Δy = 10cm.

Upper image (6a) shows image reconstructed with approach not dealing with antennas separation, and lower one (6b) shows image reconstructed with algorithm proposed. It's seen that significant distortions caused by antennas separation are almost completely eliminated with approach proposed.

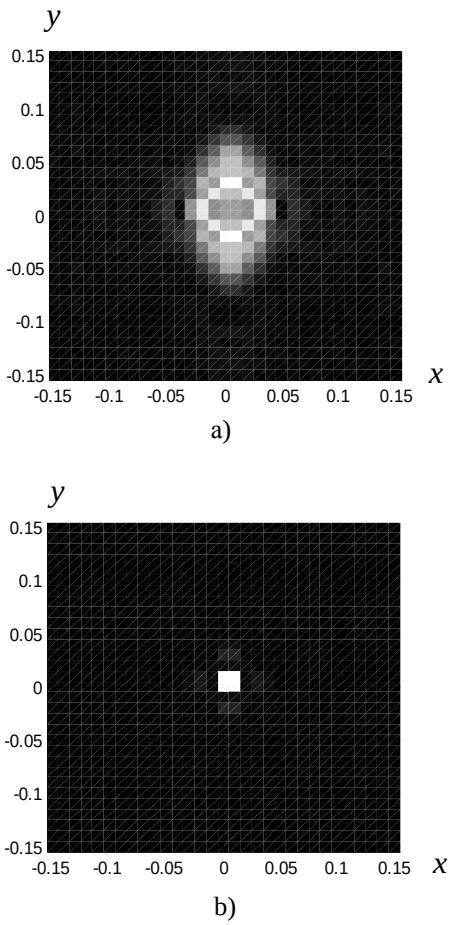

Fig. 6 Point object image reconstructed in multi-frequency case

EXPERIMENTAL RESULTS

An experimental setup described in [6] was used to test approach proposed against experimental data. System aperture has size of 32x32 points situated at 1x1 cm grid nodes; images reconstructed have the same size and resolution. The point object (small metallic disc) was put at 14 cm from the aperture plane. Eleven illuminating frequencies in 6 GHz to 10 GHz range were used. Antennas were separated along vertical axis by 20 cm (Δy = 20 cm).

Figure 7 shows images reconstructed with three approaches – without taking care of antennas displacement, with closed form frequency response and with numerical frequency response (upper, middle and lower images). It's clearly seen that ignoring antennas offset leads to inappropriate reconstruction. Using numerical frequency response shows superior image quality over closed-form frequency response, which is expectable since closed-form approach uses assumptions that are not true for this case. Still, image reconstructed with closed-form frequency response is acceptable.

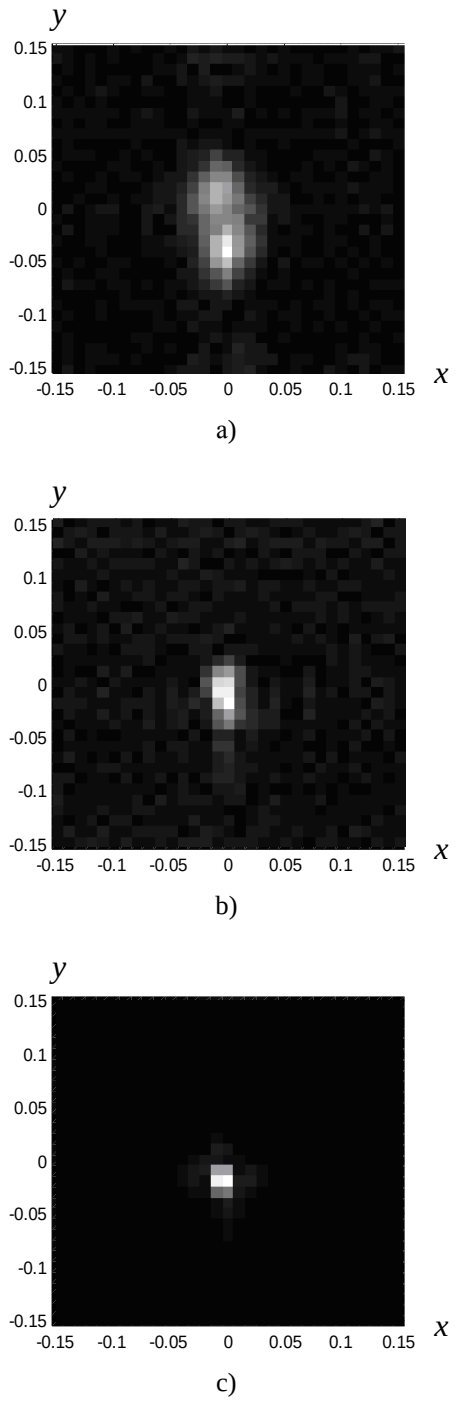

Fig. 7 Point object image reconstructed on experimental data

The approach was also tested on objects more complicated that point object. Image reconstruction results of "A" letter model are presented in figure 8. It's seen the approach is still effective under these conditions, and numerically calculated frequency response showed better performance again.

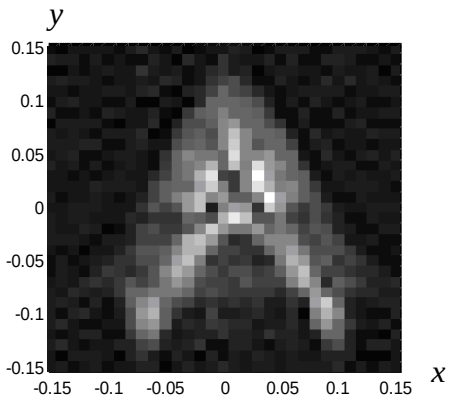

a)

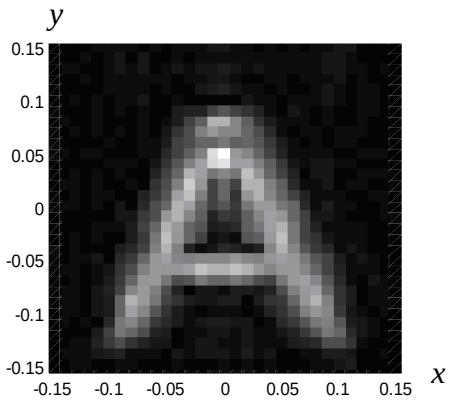

b)

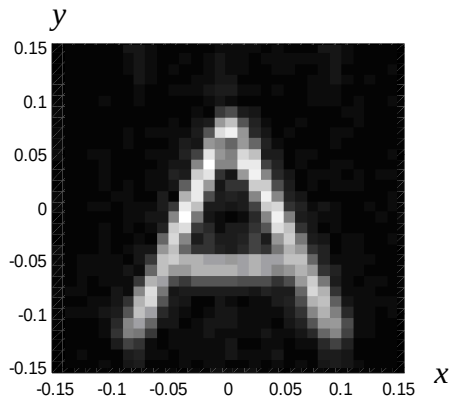

c)

CONCLUSION

An image reconstruction approach dealing with antennas separation for two-antenna scan aperture synthesis was presented. An approach is based on Born approximation and solves linearized inverse problem in frequency domain. Closed-form frequency response was obtained under certain approximations. Experimental results showed effectiveness of the approach; however, numerically calculated frequency response offered better image quality compared to closed-form frequency response.

REFERENCES

[1] G. A. Massey, "Acoustic imaging by holography." *IEEE Trans. on Sonic and Ultrasonic*, vol. 15, issue 3, pp. 141–143, Jul. 1968.

[2] V. A. Pahomov, V. G. Semenchik, and S. V. Kurilo, "Reconstructing reflecting object images using born approximation." in *Proc. 35th European Microwave Conf.*, pp. 1375-1378, Oct. 2005, Paris, France.

[3] M. G. Slaney, "Imaging with diffraction tomography (Thesis)", Ph. D. dissertation, Ph.D. dissertation, Purdue univ., Purdue, IN, 1985.

[4] A. D. Polyanin and A. V. Manzhirov, *Handbook of Integral Equations*, CRC Press, Boca Raton, 1998.

[5] V. A. Zverev, *Radiooptics*, Sov. radio, Moscow, 1975.

[6] V. G. Semenchik, V. A. Pahomov, and S. V. Kurilo, "Multifrequency microwave imaging" in *Proc. MSMV 2004*, Kharkov, Ukraine, pp. 193-195